Journal of the Atmospheric Sciences

Supplemental Material:

The linear response function of an idealized atmosphere. Part 1: Construction using Green's functions and applications

Pedram Hassanzadeh* and Zhiming Kuang†

S1 Supplementary Figures

Figure S1 The eigenvalues of $\tilde{\mathbf{M}}$ with timescales longer than 1 day.

Figure S2 $\overline{\mathbf{f}}$ for Test 2.

Figure S3 $\overline{\mathbf{f}}$ for Test 3.

Figure S4 EOF1 of $\overline{\mathbf{z}}$ which is obtained from integrating the stochastic linear equation (Eq. (18)).

S2 Supplementary Tables

Table S1 Thermal forcing amplitudes $\bar{f}_o$.

Table S2 Mechanical forcing amplitudes $\bar{f}_o$.

S3 Forcing $\overline{\mathbf{f}}$ for Tests 2 and 3

The forcings $\overline{\mathbf{f}} = -\hat{\mathbf{M}}\,\langle\overline{\mathbf{y}}\rangle$ calculated to force the specified mean-flow $\langle\overline{\mathbf{y}}\rangle$ in Tests 2 and 3 are shown in Figs. S2 and S3. The thermal forcing for Test 2 includes heating in the high-latitudes mid-troposhere, which more or less coincides with the region of the positive temperature response (Fig. 2(b)). The mechanical forcing pattern is more complex and its main feature is a strong easterly torque in upper troposphere/lower stratosphere to the south of the region of equivalent-barotropic easterly zonal-wind response (Fig. 2(a)).

For Test 3, again the thermal forcing to some extent resembles the targeted temperature pattern (Fig. 3(b)) and includes heating in the midlatitudes and cooling in the high-latitudes. The mechanical forcing pattern is again more complex and includes a strong westerly (easterly) torque

*Center for the Environment and Department of Earth and Planetary Sciences, Harvard University, Cambridge, Massachusetts, USA

†Department of Earth and Planetary Sciences and John A. Paulson School of Engineering and Applied Sciences, Harvard University, Cambridge, Massachusetts, USA.

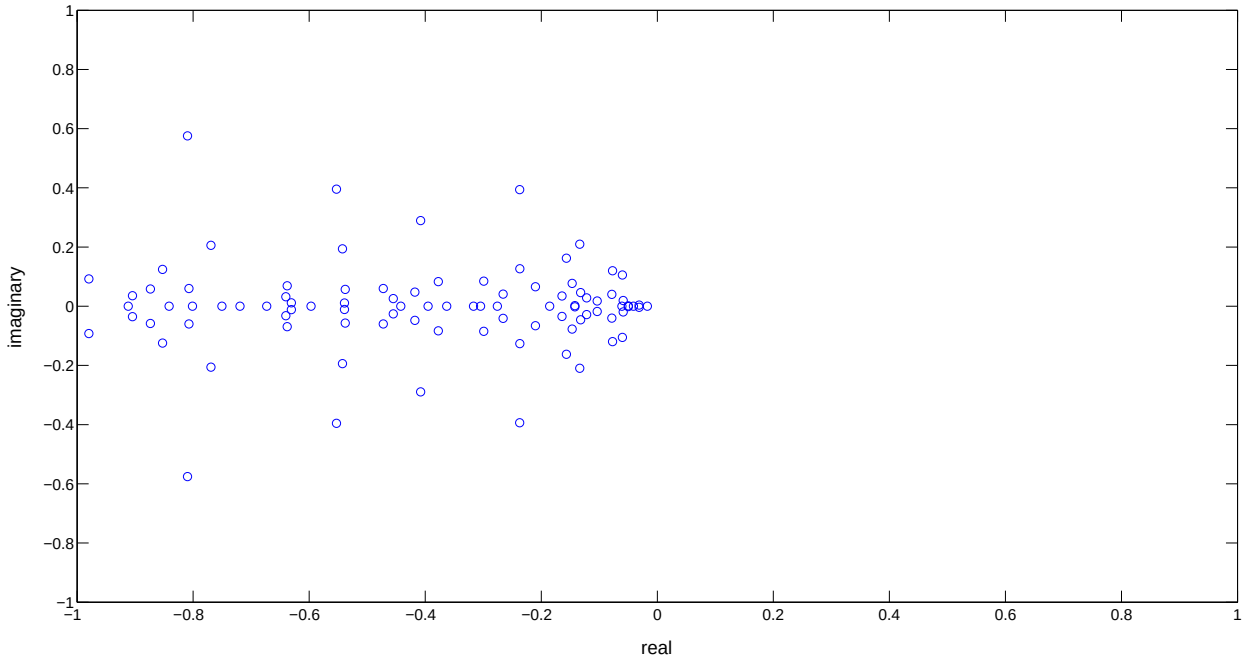

Figure S1: The eigenvalues of $\tilde{\mathbf{M}}$ (calculated from Eq. (13)) with timescales longer than 1 day. The horizontal (vertical) axis shows the real (imaginary) part of the eigenvalues. The eigenvalues are either real and negative, or pairs of complex conjugates with negative real parts. The eigenmodes of some of the slowest decaying modes are shown in Fig. 6.

concentrated in the upper troposphere to the south (north) of the region of equivalent-barotropic westerly zonal-wind response (Fig. 3(a)).

The implications of these two forcing patterns for the relationship between forcing and mean-response should be treated with caution. This is because these forcings might still contain components that correspond to the fast and inaccurate modes despite the filtering (14). However, when these forcings are applied in the GCM, these components only affect the transients and not the mean-response. Note that the forcing needed to force the neutral vector (Figs. 5(c)-5(d)) is the optimal forcing and provides a more reliable example for the relationship between the forcing and mean-response.

This issue can be further illustrated using the forcing calculated for Test 2 (Fig. S2). The 10% change in the Newtonian relaxation timescale results in a purely thermal forcing. This forcing can be analytically calculated and its pattern and amplitude are fairly similar to the thermal component of the forcing computed using $\hat{\mathbf{M}}$ (Fig. S2(b)). However, the forcing calculated using $\hat{\mathbf{M}}$ also has a mechanical component (Fig. S2(a)), which is due to the fast and inaccurate modes of $\hat{\mathbf{M}}$. Applying the mechanical and thermal components of the forcing to the GCM separately shows that while the response to the mechanical forcing alone is weak and has a pattern that is different from the pattern of the target, the pattern and amplitude of the response to the thermal forcing alone is quite similar to those of the target (still, the relative errors of zonal-wind and temperature are both around 16%, which are twice larger than the errors when the two components are applied together).

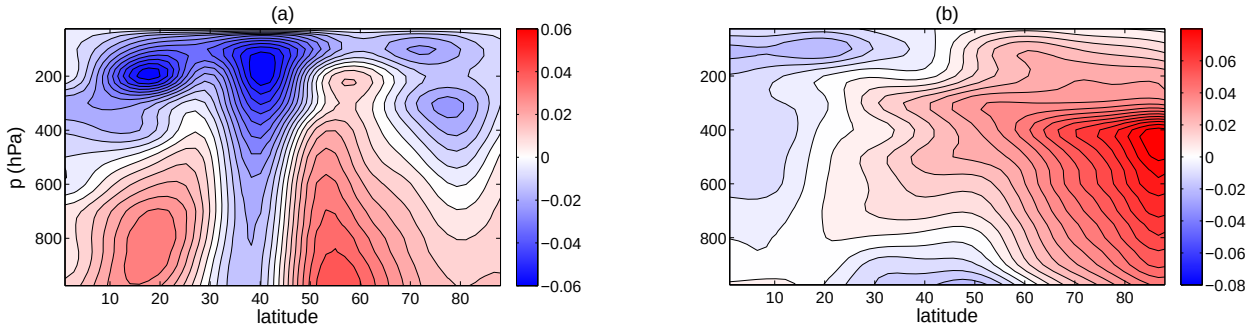

Figure S2: Forcing $\overline{\mathbf{f}}$ calculated to force the specified mean-flow of Test 2: (a) mechanical component (forcing of zonal-wind) in m s^{-1} day^{-1}, (b) thermal component (forcing of temperature) in K day^{-1}.

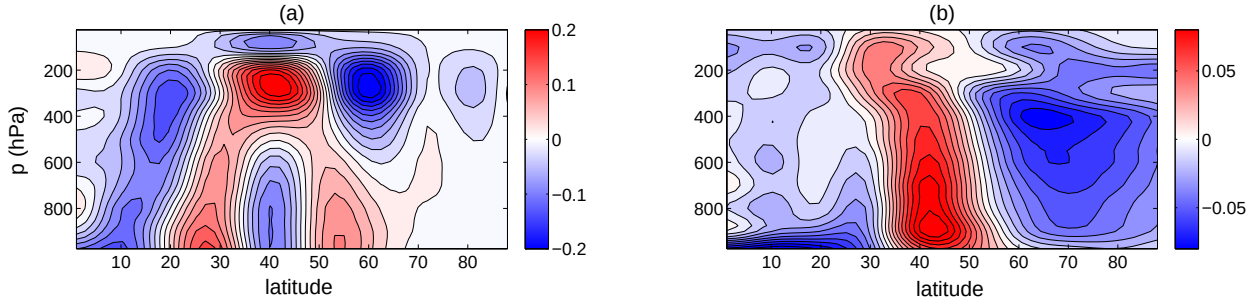

Figure S3: Forcing $\overline{\mathbf{f}}$ calculated to force the specified mean-flow of Test 3: (a) mechanical component (i.e., forcing of zonal-wind) in m s^{-1} day^{-1}, (b) thermal component (i.e., forcing of temperature) in K day^{-1}.

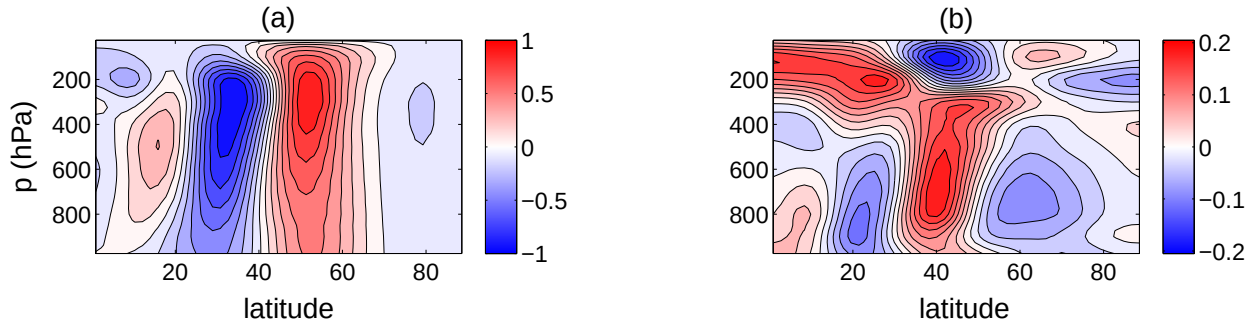

Figure S4: The leading EOF (EOF1) of $\overline{\mathbf{z}}$ which is obtained from integrating the stochastic linear equation $\dot{\overline{\mathbf{z}}} = \hat{\mathbf{M}}\,\overline{\mathbf{z}} + \boldsymbol{\zeta}$ for 15 million days. See section 5 of Part 2 (Hassanzadeh and Kuang 2016) for details. $\boldsymbol{\zeta}(t)$ is Gaussian white noise and $\langle \boldsymbol{\zeta}\boldsymbol{\zeta}^{\dagger} \rangle = \mathbf{I}$. EOF1 explains $\sim 38\%$ of the total variance. The (a) zonal-wind in m s^{-1} and (b) temperature in K of EOF1 strongly resemble the neutral vector of $\hat{\mathbf{M}}$ (Fig. 5).

Table S1: Thermal forcing amplitudes $\bar{f}_o$ in K day^{-1} for every (μ_o, p_o) used in calculation of $\hat{\mathbf{M}}$ and $\hat{\mathbf{E}}$.

$p_o \diagdown \mu_o$	0	10	20	30	40	50	60	70	80	90
100	0.1	0.2	0.2	0.2	0.2	0.2	0.2	0.25	0.2	0.2
200	0.1	0.1	0.1	0.1	0.1	0.1	0.1	0.2	0.3	0.2
300	0.1	0.1	0.1	0.1	0.1	0.2	0.25	0.2	0.3	0.5
400	0.1	0.1	0.1	0.1	0.1	0.3	0.2	0.2	0.4	0.4
500	0.1	0.1	0.2	0.1	0.2	0.4	0.2	0.2	0.4	0.5
600	0.2	0.2	0.2	0.3	0.175	0.2	0.2	0.2	0.5	1.0
700	0.2	0.2	0.2	0.1	0.1	0.3	0.2	0.2	0.5	1.0
800	0.3	0.2	0.2	0.2	0.2	0.3	0.2	0.3	0.6	1.75
900	0.2	0.35	0.2	0.2	0.4	0.3	0.4	0.4	0.8	2.5
1000	1.0	0.9	0.6	0.7	0.9	0.7	0.5	0.8	1.25	3.5

Table S2: Mechanical forcing amplitudes $\bar{f}_o$ in m s^{-1} day^{-1} for every (μ_o, p_o) used in calculation of $\hat{\mathbf{M}}$ and $\hat{\mathbf{E}}$.

$p_o \diagdown \mu_o$	0	10	20	30	40	50	60	70	80	90
100	0.025	0.025	0.15	0.6	0.4	0.8	0.8	1.0	1.0	1.5
200	0.1	0.2	0.4	0.6	0.9	0.8	0.8	1.0	1.25	1.5
300	0.2	0.2	0.4	0.6	0.9	0.7	0.8	1.0	2.0	1.5
400	0.3	0.5	0.4	0.6	0.9	0.7	0.8	1.0	1.75	1.5
500	0.3	0.3	0.5	0.6	0.7	0.7	0.8	1.25	2.0	2.5
600	0.3	0.3	0.5	0.8	1.0	0.7	1.0	1.25	1.5	2.5
700	0.4	0.4	0.5	0.6	1.0	0.7	1.0	1.25	1.75	2.5
800	1.0	0.6	0.5	1.25	1.5	1.0	1.0	1.5	2.0	3.0
900	2.5	1.25	1.25	1.5	1.5	1.5	1.5	1.5	2.0	3.5
1000	3.0	2.0	2.0	2.0	2.0	2.0	2.0	2.0	3.0	4.0